

Title:

Part VI: Quantum Mechanics and Physisorption - Mesoporosity

Author: James Condon^{*†}

Professor Emeritus

*Prof. Emeritus for the Regents College and Universities of the State of Tennessee, Roane State Community College, and former Senior Staff Member (Chemistry Research and Development) Oak Ridge Laboratories and adjunct full professor at University of Tennessee, and Gast Wissenschaftler Forschung Zentrum Juelich DE.

† Corresponding author. Email: condonjb@genchem.net

© Copyright - October 2024 by James B Condon all rights reserved.

revised: 09.Jan, .2025

Contents

Abstract	2
Introduction	3
Calculating Mesoporosity: Volume, Area and Pore Size Distribution:	3
Recognizing Mesoporosity	4
Fitting mesopore isotherms – the D function again and a new function χ^1	5
Example 1 – N ₂ adsorbed on silicas (KIT-6):.....	7
The Desorption branch calculated from the Adsorption branch.	9
Example 2 The peak for mesoporosity GWMTK SBA-15 silica:.....	11
Speculation about calculating hysteresis:	14
Conclusion concerning mesoporosity:	16
What is next?	16
Appendix I about equations 1 and 2:	16
References:	18

Keywords: Physisorption, Quantum Mechanics, BET Theory, physical adsorption, micropores, mesopores

Abstract

The determination of the parameters for mesoporosity requires knowledge from the previous parts for this series. The basic equation is that obtain with the creation of the χ -plot and the $\Delta\chi$ -plot and the log-law-plot. Compensation for the heterogeneity is needed to get the best resolution but may be bypassed by beginning above the value for $n_a = 0$. However, this might insert undesirable uncertainty in the calculation and, if the equipment is capable, data should be obtained at least into the HV and preferably in the UHV. Regardless of the initial appropriate plot, the mesoporosity is a modification using the cumulative normal distribution, **D**, or the inverse χ -function, χ^{-1} , for the simple case of one type of mesoporosity. If there is microporosity, the two might be separated enough from each other that an analysis is possible.

The mesoporosity is calculated by inserting function **D** or χ^{-1} into the calculation. Both the adsorption and desorption may be analyzed this way. Often, hysteresis accompanies mesoporosity. It is too early in the development to claim this can be predicted. Suggestions are provided for a possible explanation. However, the only certainty is that the use of the **D** or χ^{-1} function provides a very good fit to a simple case. If there are more than one size of mesoporosity with a broad distribution, a more sophisticated least square method might separate the sizes. The possible origins for hysteresis is presented with example calculations.

Main text:

Introduction

So far in Parts I through V. the following has been addressed:

Part I The absolute disproof for various isotherm equations, including the BET, was presented. This provides reason for the search for new hypotheses of physisorption to be brought forth.

Part II A list of experimental problems and processes is provided. The definition of the thermodynamic system is clarified and the common experimental errors in the literature are listed. These errors are very common with the popular commercial instruments, so advice is provided as to how to overcome these errors with minor modification.

Part III This part goes into more detail about the BET and provides a possible way to use the two parameters of the BET to recalculate the quantum mechanical output parameters from them. It also demonstrate why the ordinate transform for the BET graphical analysis method is mathematically invalid. Furthermore, the standard deviations are incorrect regardless of how it is arrived at. Use of a nonlinear least square eliminates the internal BET error, but the BET itself is wrong. Never-the-less, a method is presented that correlates the BET answer with the QM. Of course, if one still has the original data, it can be recalculated using QM equations.

Part IV The resultant equations for QM hypothesis analysis are derived. This derivation is a general treatment and results in a universal equation used by others in the past as an empirical equation. However, the empirical equation has never been used to provide the proper energies and monolayer equivalence that are the point of the analysis. On the other hand, the QM seems to be quite universal for all numbered “Types” of isotherms except those that are obtain below the freezing point of the adsorbent. The QM It also provides a method of calculating the occupation of the admolecules densities in the various schichten (or “layers”) of adsorption. The hypothesis “Excess Surface Work” of ESW, a confirmatory hypothesis, is also introduced.

Part V The analysis of microporosity is provided with a special form of the QM schichten equations. This form is called the “log-law” as applied to a monolayer adsorption. Analysis of additional schichten is provided with some examples.

Part VI addresses mesoporosity including hysteresis

What is left to address in Part VII is calorimetric calculation and the relationship to the isotherm. The final section addresses binary adsorptive adsorption, which is very tentative since high quality data for testing is mostly missing.

Calculating Mesoporosity: Volume, Area and Pore Size Distribution:

There is no question that the QM characterization is easy to do and easy to interpret compared to other techniques. However, the important question of prediction has not yet been addressed. It seems probable that a combination of QM and ESW will yield some answers.

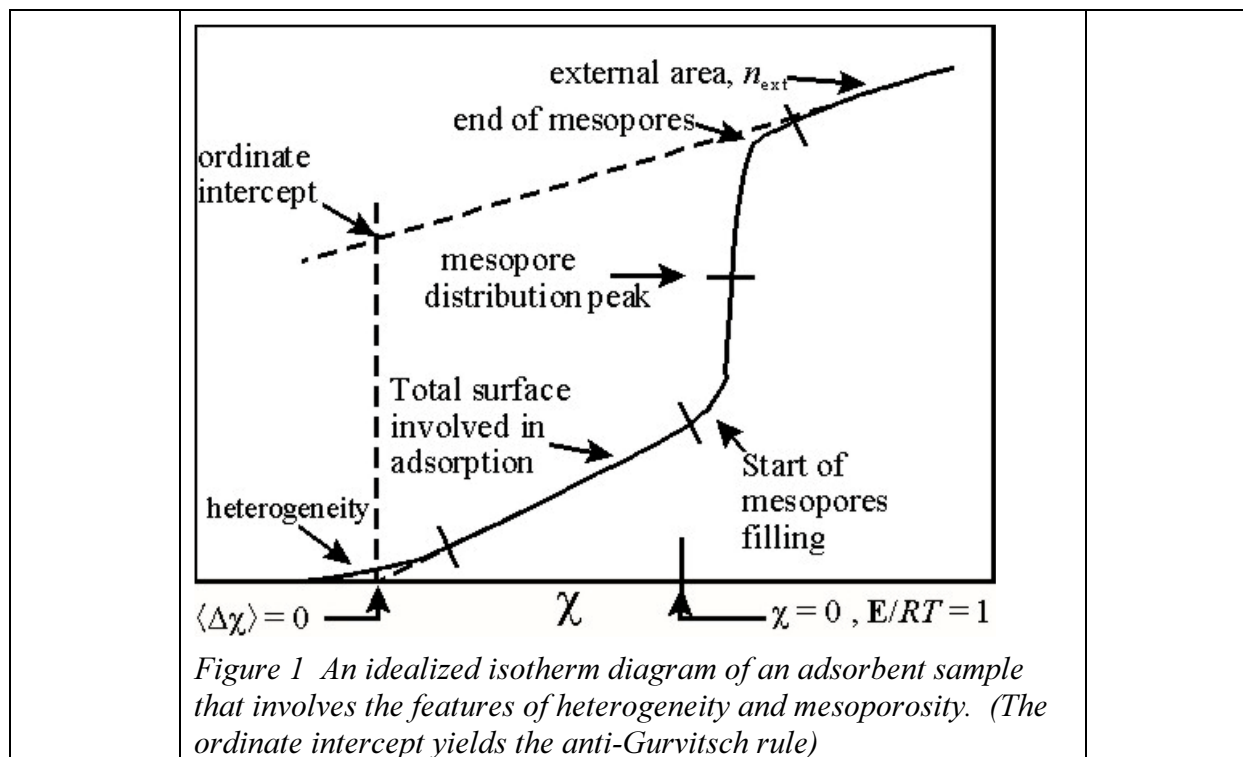
In previous sections, the definitions of physical adsorption with the use of the QM formulation does not necessarily follow the SIO/IUPAC definitions. The IUPAC definitions of micropores and mesopores were classified according to the radius or pore wall separation. For the modern

definitions, this is replaced by questions of what the interactions are between the adsorbent and adsorbate. This interaction is between E for the pore radii and the $\Delta^a E$. It is therefore based upon competing energies that determine the classification of micropore versus mesopore.

Recognizing Mesoporosity

Mesoporosity is characterized by a positive curvature in the χ -plot followed by a negative curvature. This usually results in a final linear portion for the χ -plot, which has a slope less than the beginning slope. This is assuming that there are no other features that complicates the analysis. This feature begins normally at $\chi \geq 0$ ($-\Delta^a E/RT \leq 1$ or $P/P_{\text{vap}} \geq 0.38$.) This value of χ is due to the energy considerations and not to the fact that it is the inflection point. A typical isotherm with these possible features are shown in *Figure 1* for multilayer isotherms.

For nitrogen the energy for at $\chi = 0$ at 78 K is -648 J mol^{-1} . One expects for the typical mesopore radii that the transition for mesoporosity onset is at a little higher value, perhaps about -300 J mol^{-1} (Remember, think exothermic.) However, for other adsorptives, such as water or benzene, this may not be the case.



If the pore filling calculates a value of $\Delta\chi < 2$, it might mean that hysteresis is not possible, since at least between 2 and 3 monolayer equivalence locally is needed to complete the gas liquid interface.

The hysteresis may be an artifact of a shifting E_a , but also not always. It seems to be the case that for some hysteresis loops they disappear when one plots $\Delta\chi$ instead of χ . This could make

sense if the onset of pore filling is due only to competing energies since χ is a measure of internal energy, The reason for the shift is unclear, but $\Delta\chi$ is affected by any shift in P_c .

There has been much discussion about the origin of hysteresis in literature, but for this section only the question of where the mesoporosity begins is addressed. This section does not explain mesoporosity, neither why it starts for adsorption nor why there is hysteresis for desorption. Speculation will be presented after how to fit it experimentally to yield the relevant parameters. Once one has these parameters, than perhaps a reasonable mechanism can be demonstrated.

*Fitting mesopore isotherms – the **D** function again and a new function χ^1 .*

The approach that is presented in this section is for fitting mesoporosity is as follows:

The first task is to characterize the mesopore phenomenon with a reliable equation. If the isotherm indicates two or several distinct isotherm onsets, then they are analyzed as separate isotherms as demonstrated in Part II. If not, then a distribution of E_{as} is the obvious conclusion.

However, the distribution of E_{as} is not relevant in a χ -plot, only but only in a $\Delta\chi$ -plot. The reason is that χ value is the value of $\Delta^a E$ for all the isotherms in the entire manifold. Thus, even though the individual isotherms within the distribution differ in starting E_{as} , they are added at the point at which they have identical $\Delta^a E$. This implies that if there is a distribution for the mesopore filling, it is due to a distribution of pore sizes or shapes randomly over a range. and not on the adsorbent heterogeneity. If nature is bias toward the normal distribution and if there are a variety of pore sizes and shapes, then the **D** function would apply to the mesopore feature. This additional feature is expressed in

Equation 1.

$$\mathbf{n}_a = \mathbf{n}_{a,i} + (\mathbf{n}_{a,f} - \mathbf{n}_{a,i}) \mathbf{D}(x, \langle x_p \rangle, \sigma_p) \quad \text{Equation 1}$$

where: $\mathbf{n}_{a,i} = (\Delta\chi n_m)$ and $\mathbf{n}_{a,f} = (\Delta\chi n_{ext} + n_p)$

Also, the following are the symbols used:

From here on the subscript “p” will be used to indicate either the χ_p , $\Delta\chi_p$ or $\mathbf{E}(\chi_p)$, depending on choice, of the peak position of the distribution function for the pores. This subscript will also apply to the description of the distribution of the pores so: $1\sigma_p$.

x can be either $\Delta\chi$ or χ depending upon preference.

D is the normal cumulative distribution, $x_p =$ value,

$\langle x_p \rangle =$ the peak of the pore distribution, **G**, which is the differential of **D**.

$\sigma_p =$ standard deviation (spread of **G**)

$\mathbf{n}_{a,i}$ is the amounts amount of \mathbf{n}_a in the initial portion of the isotherm before mesopore filling is evident, and $\mathbf{n}_{a,f}$ is the final amount after the filling. (This is assuming one type of pore. With several types one would have an initial and final portion for each type.)

The n_s are written as functions of either $\Delta\chi$ or χ and are, therefore, in bold.

There is an alternative to *Equation 1*. This is the inverse χ -function, χ^1 .

$$\mathbf{n}_a = \mathbf{n}_{a,i} + (\mathbf{n}_{a,f} - \mathbf{n}_{a,i}) \exp \left\{ -\exp \left(-\frac{(x - \langle x_p \rangle)}{\sigma_p} \right) \right\} \quad \text{Equation 2}$$

$\langle x_p \rangle$ (x_p for short) in this case is the peak value and not the mean. The equation is related to the **D** function. Instead of squaring the inner argument, it is taken to the limit ∞ . It is slightly skewed with a peak. For sharp peaks this yields lower overall standard deviation, but for broad peaks the opposite seems to be the case. Many more experiments are needed to determine the usefulness of each.

For desorption the mirror image of the χ^{-1} function can be used:

$$\mathbf{n}_a = \mathbf{n}_{a,f} + (\mathbf{n}_{a,i} - \mathbf{n}_{a,f}) \exp \left\{ -\exp \left(\frac{(x - \langle x_p \rangle)}{\sigma_p} \right) \right\} \quad \text{Equation 3}$$

However, the important parameter $\langle x_p \rangle$, does not change, since the differences in the distribution are very low on the “wings” of the distribution. See Appendix I for further explanation about these functions. The **D** function is symmetrical, so its mirror image is the same.

All this assumes that heterogeneity and mesoporosity do not overlap¹. At the moment this seems unlikely because it appears that the mesoporosity is confined to be after the Fuller magic point, $P/P_{\text{vap}} = 1/e$, and other forms of porosity* are prominent before the magic point. Thus, if there is heterogeneity, then the values for n_a are calculated by the positive heterogeneity **Z** function, (See Part II - Heterogeneity). These values for n_a (now designated \mathbf{n}_a , $\mathbf{n}_{a,i}$, and $\mathbf{n}_{a,f}$) are modified by multiplying by the function for mesoporosity, in

Equation 1 .

If only one heterogeneity and one type of mesoporosity is present, then the final slope of $\mathbf{n}_{a,f}$ in the equation yields the external monolayer equivalence. Furthermore, extrapolating $\mathbf{n}_{a,f}$ back to $\Delta\chi = 0$ yields the pore volume, n_p in term of moles, (the anti-Gurvitsch rule or the *ordinate* intercept for the extrapolated $\mathbf{n}_{a,f}$ in the $\Delta\chi$ -plot to yield n_{ext}^\dagger .)

Obviously, these 3 new mesopore parameters, along with the 3 heterogeneous parameters[‡] are best determined with a non-linear least squares routine. With heterogeneity and mesoporosity there are now 6 parameters. This includes the 3 parameters for $\mathbf{n}_{a,i}$ of n_m , $\langle \chi_\zeta \rangle$ and ζ and the 3 parameters for the switch to $\mathbf{n}_{a,f}$ of σ_p , $\langle \chi_p \rangle$ (or $\langle \Delta\chi_p \rangle$) and n_{ext} . In general, each feature adds 3 parameters.[§]

Up to this point there is no supported hypothesis to specify the meaning of $\langle \chi_p \rangle$ nor σ_p other than as fitting parameters. Obviously, σ_p is an indication of the distribution of pore cross-section

* This includes monolayer restricted adsorption and other low schicht restricted fillings. See Part V for examples.

† the ordinate for the log-law.

‡ Of course, if the plot does not approach $n = 0$, the heterogeneity cannot be measure and one has 2 parameters

§ Recall that ζ might be missing due to lack of low-pressure data and if a least square routine is used, it needs to be set of a very low number because 0 causes a computation error. If you then activate ζ and it is negative that may mean you have detected the Knudsen effect.

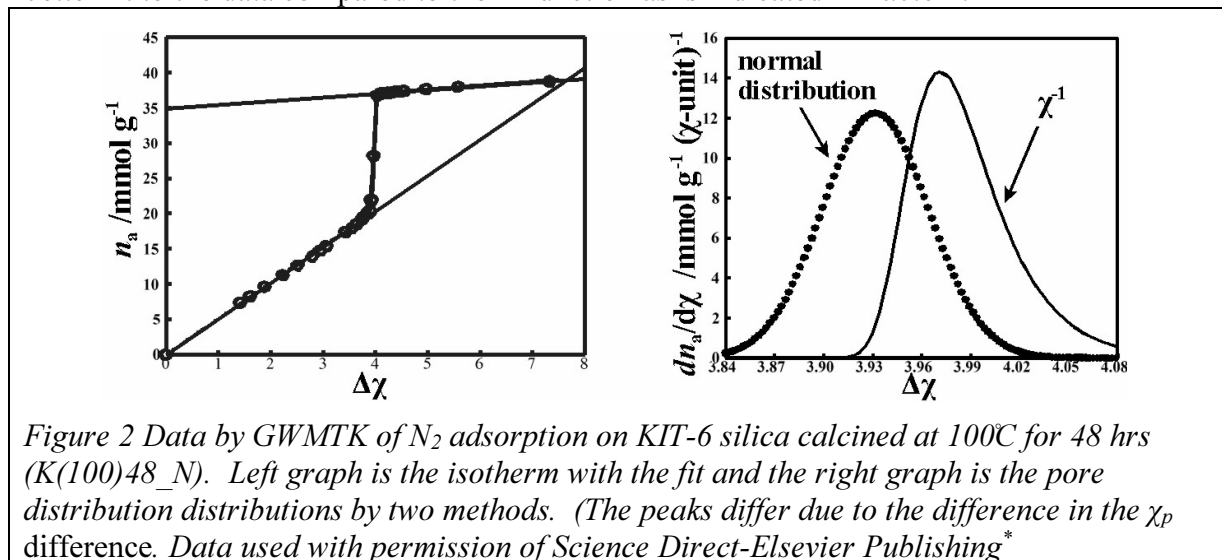
areas, since the total pore volume is already determined by the anti-Gurvitsch rule. The position of $\langle\chi_p\rangle$ is probably a trade-off in energies $\Delta^a E(\chi)$ versus $A_p \gamma_{lg}$ for a curved surface. This is addressed in the following section. This speculation will be presented after some examples of the fitting. Fitting the isotherm with a realistic analytical equation that has a low standard deviation helps in the interpretation.

Example 1 – N₂ adsorbed on silicas (KIT-6):

This following is an example of a mesopore fit by Guillet-Nicolas, Wainer, Marcoux, Thommes and Kleitz²(GWMTK) and is KIT-6 that was calcined at 100°C for 48 hrs. This was not measured below one monolayer equivalence. Unfortunately, this is typical, but some insight can still be obtained even though there is uncertainty about the value of χ_s . It apparently has one pore size. The adsorptive is N₂ at 78 K.

The data and the fit using χ^{-1} are shown in *Figure 2*. The graph on the left is for the entire isotherm. The graph on the right is for the distribution of pores enlarged. The fits fulfill the requirement that the standard deviation be lower than 1% of the full data range (FDR.) The standard is met here at 0.50%. The anti-Gurvitsch rule, which is the extrapolation to the ordinate of the $\Delta\chi$ -plot. (The other QM extrapolation to an ordinate is for of the log-law plot for the filling of the 1st schicht, $n_{a,1}$.)

The inverse chi function, χ^{-1} is used for the pore distribution. In this case it yields only a slightly better fit to the data compared to the **D** function as is indicated in *Table 1*.



All the parameters, standard deviations and derived quantities from the χ fits are presented in *Table 1*.

In comparison of the data, there is not much difference between the normal distribution assumption and the χ^{-1} assumption. The method and the quality of the data is good enough to detect this difference. The χ^{-1} assumption yields a better fit, but it could be doubtful that this is

* Since this peak is very sharp, one can detect a slight difference in the peak values between χ^{-1} and **D**

significant. If the pores were homogeneous it would probably be even better, but as it is a distribution of nearly normal distributions, this yields approximately another normal distribution with the peak value representing the peak energy.

In *Table 1* are the output parameters of a non-linear least squares fit to this data.

<i>Table 1 Fitting parameters for GWMTK data (K(100)48 N).</i>		
	Using the χ^1 distribution	Using the normal distribution, D
$n_m =$	5.099 mmol g ⁻¹	5.167 mmol g ⁻¹
$\chi_s =$	-2.685	-2.656
$n_{ext} =$	0.552 mmol g ⁻¹	0.505 mmol g ⁻¹
$\Delta\chi_p =$	3.971	3.933
$n_p =$	34.887 mmol g ⁻¹	34.176 mmol g ⁻¹
$\sigma_p =$	0.0257	0.0326
Goodness of the fits		
$\sigma_{fit} =$	0.193 mmol g ⁻¹	0.247 mmol g ⁻¹
σ_{fit} (FDR)=	0.497 %	0.635 %
Derived quantities:		
$E_a =$	9.51 kJ mol ⁻¹	9.25 kJ mol ⁻¹
$E_p =$	179 J mol ⁻¹	181 J mol ⁻¹
$V_p =$	1.01 mL(ρ_l) g ⁻¹	1.02 mL(ρ_l) g ⁻¹
A_p (IUPAC) =	444 m ² g ⁻¹	404 m ² g ⁻¹

To obtain measurements that are not confined to moles but rather meters there needs to be some conversion factors used. Furthermore, now, there is no settled way in QM to calculate the desorption branch of the hysteresis loop, in spite of the speculation below. Some possibilities seem logical:

- 1) The value for χ_s shifts, perhaps from level of surface contamination changing or
- 2) The geometry of the pore liquid-gas interface changed, for example from a 1D curvature to a 2D curvature affecting the parameter m in *Equation 4* below³.

It may be that both phenomena and perhaps others are occurring. These other factors might be revealed with further research. This seems to be a fertile area of physisorption for research.

The Desorption branch calculated from the Adsorption branch.

One of the discoveries that the QM model presented is the importance of the E_a in the calculation of the desorption isotherm. Firstly, the E_a is the zero point for the n_a , whereas $\chi = 0$, is the reference point for an energy. $\chi = 0$ is the inflection point regardless of what the starting point for the isotherm is. Furthermore, the slope of the untransformed isotherm at that point is n_a . This has been referred to earlier as the Fuller “magic point.” At the “magic point” $P/P_{vap} = 1/e$ or 0.3678... and the QM energy $\Delta^{\#}\bar{E} = 648 \text{ J mol}^{-1}$ at 78 K. The magic point is the reference to

compare the mesopore peaks using difference in χ from this point. The distance from $\chi = 0$ to the adsorption mesopore peak and the desorption mesopore peak should be equal, if there is the same energy of transition. Even though they appear different in the untransformed isotherm, often they are not in the QM transform. The shift in the peak of the mesopores is due to the (sometimes undetectable) shift of in the extrapolated E_a which applies immediately before the peaks and might be evident at least after $\chi = 0$. A shift before $\chi = 0$ may be consistent with the shift after $\chi = 0$ but may not be necessary to create this phenomenon.

There is a concept called thickness in physisorption with the symbol “ t .” This letter is used for the quantum mechanic and for ESW, but the meaning is slightly different. “ t ” for ESW is in the classic meaning with liquid trapped between two definite interfaces, the liquid-gas (lg) and liquid-solid (ls) interface, that has some structural strength. However, for QM it is the sum of all the areal densities of the adsorbate in the schichten that are allowed, that is, $\Sigma n_{a,n}$ from $n=1$ to the highest allowed by geometry.

Here are some definitions used;

r_c := radius from one adsorbate-adsorptive boundary to the center of the pore and

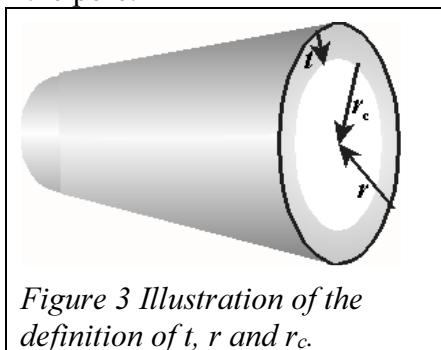
t := distance from the adsorbent wall to the adsorbate-adsorptive interface

r := pore radius from the adsorbent wall to the center of the pore.

Thus, $r_c = r - t$.

(See Schematic in *Figure 3*.)

By convention then $t \geq r_c \geq 0$ and when $r_c = 0$, the pore is full. In other words, in classical terms, r_c is the vacant cylinder within the pore.



A conversion from monolayer thickness to SI is needed for this to be useful. By the IUPAC convention this would be $t_m = 0.354 \text{ nm}$ for N_2 and sometimes given the symbol λ .

Other symbols used are:

m = a geometric factor, which is $m = 1$ for a film that has one concave surface, or

$m = 2$ for a film that has two concave surfaces, or something else for a variety of reasons.

γ_{lg} = surface tension of adsorbate for the liquid gas interface

\bar{V} = molar volume of adsorptive liquid

The subscript “ $p\uparrow$ ” may be used without conflict to indicate the mesopore onset peak for adsorption, and “ $p\downarrow$ ” for the desorption branch.

Example 2 The peak for mesoporosity GWMTK SBA-15 silica:

One should be able to calculate pore size with knowledge of the surface tension of the adsorptive and the value of χ for the mesopore peak. In the GWMTK case in *Figure 4* the adsorptive is N_2 at 78 K and the adsorbent is SBA-15 calcined at 413 K for 24 hours (S(140)24_N.) The following constants were used:

$$\gamma_{lg,78K} = 8.72 \text{ mN m}^{-1}, \rho_{N_2(l)} = 0.809 \text{ g mL}^{-1} \text{ implying } \bar{V}_{N_2(l)} = 34.63 \text{ mL mol}^{-1}.$$

The nitrogen surface tension at 77K is from the UNIFAC (Dortmund) data base⁴ with several authors in agreement.

Equation 4 is useful for calculating the radius from the energy and vis-a-versa. These assume the Kelvin (Ostwald–Freundlich form converted to energy) . However, modifications to this equation may be warranted.

$$\langle E_p \rangle := \Delta_l^a \mathbf{E}(\chi_p) = -\frac{m\bar{V}\gamma}{r_c} \quad \text{or} \quad r_c = -\frac{m\bar{V}\gamma}{\langle E_p \rangle} \quad \text{Equation 4}$$

(Recall E_s are negative, exothermic.)

This GWMTK sample was chosen because the graphs were reasonably readable and enough data points present in critical areas. The isotherm and the pore size analysis is presented in *Figure 4* and *Figure 5* A summary of the output data and derived quantities is presented in **Table 2**. In the NLDFT results by GWMTK is also presented for comparison. The spread in the NLDFT is much larger in the pore distribution than the QM results. However, the NLDFT assumes a hard core for the admolecules that should spread out the looks of the distribution, whereas the QM calculation is center-to-center.)

In *Figure 4* the calculation of the QM pore distribution used both the **D** distribution and the χ^{-1} distribution. In *Figure 5* the **N** companion distribution of the **D** function is the \times 's line. The solid line is the χ^{-1} distribution. There is slight difference between the two.

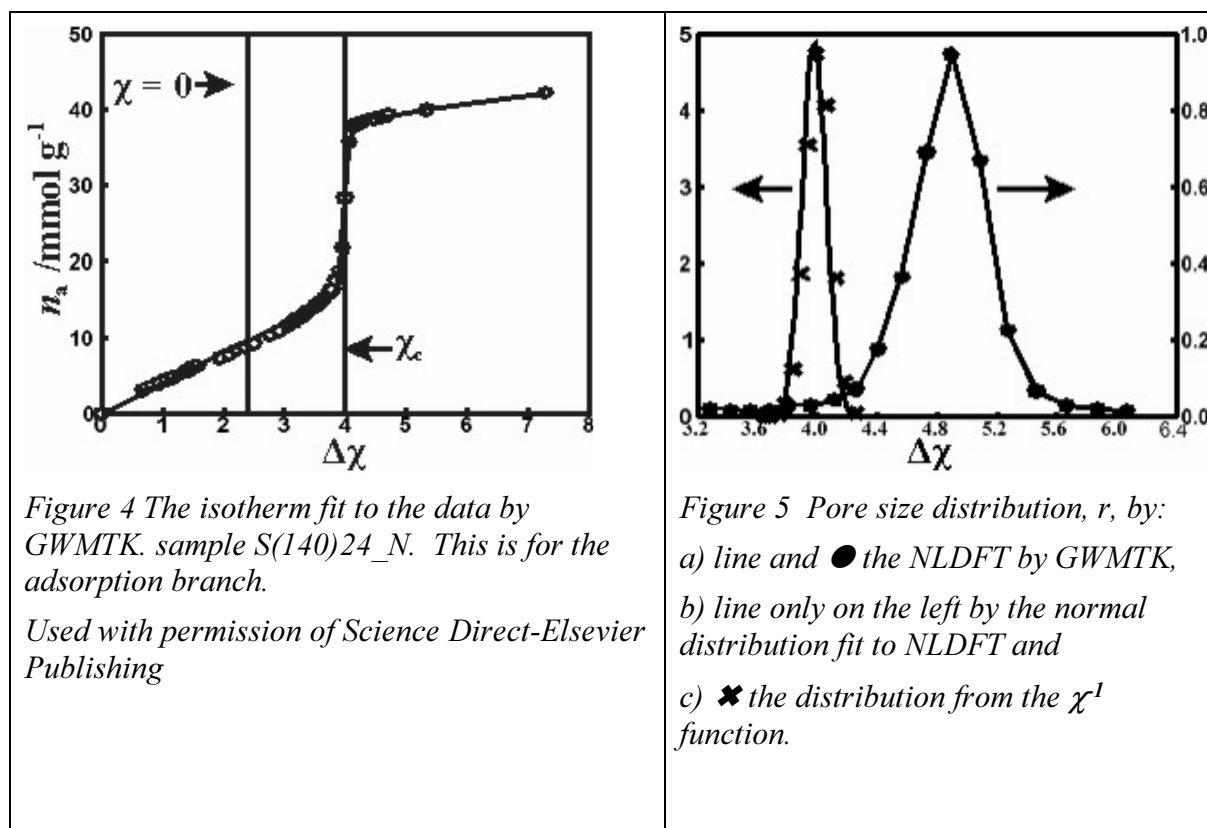


Figure 4 The isotherm fit to the data by GWMTK. sample S(140)24_N. This is for the adsorption branch.

Used with permission of Science Direct-Elsevier Publishing

Figure 5 Pore size distribution, r , by:
a) line and \bullet the NLDFT by GWMTK,
b) line only on the left by the normal distribution fit to NLDFT and
c) \times the distribution from the χ^1 function.

In Table 2, the conversion to SI units uses the classical IUPAC conversions listed in the physical adsorption conventions^{5,6}. For example, nitrogen has the classical molar area of $9.77 \times 10^4 \text{ m}^2 \text{ mol}^{-1}$, and the conversion from linear monolayer equivalence is IUPAC classical diameter of $0.354 \text{ nm monolayer}^{-1}$. (Opposing sides, however, need to be counted.) (The van der Waals $d = 3.1 \text{ nm}$ and the following dimensions apply to solid N_2 : the waste is $d_w = 0.339 \text{ nm}$ and the length is $d_l = 0.434 \text{ nm}$. Thus classically, it makes a 20% difference the orientation of N_2 to the surface.)

The QM analysis does not predict that an outer liquid-gas boundary exists, at least in its present development. However, we know that it happens, and if it is a sudden enough formation, then there should be a peak in the observed ΔH to indicate this. If the adsorbent is perfectly smooth, it may be that the transition is above a high θ value (≥ 9 monolayer equivalence,) thus little heat is emitted and it is not noticed. (So far, some smooth surfaces have absorbed up to 8 monolayer equivalences without any sudden shift as otherwise predicted by Brunauer^{7,8}.) Most likely, the sample becomes noticeably “wet.” This ends the experiment with adsorptive dripping off the side of the sample tube.

In Table 2 are the output parameters for the fit to this sample.

Basic values and units from QM derivation.			derived from QM ⁽¹⁾ or UPAC convention ⁽²⁾		
$n_m =$	3.979*	mmol g ⁻¹	$A_m =$	388.7	m ² g ⁻¹ ^(1,2)
$\langle \chi_s \rangle =$	-2.4163*		$\langle \bar{E}_a \uparrow \rangle =$	-7.27	kJ mol ⁻¹ ⁽¹⁾
$n_{ext} =$	1.071*	mmol g ⁻¹	$A_{ext} =$	104.6	m ² g ⁻¹ ^(1,2)
			$A_{p\uparrow} = A_m - A_{ext} =$	284.1	m ² g ⁻¹ ⁽²⁾
$n_{p\uparrow} =$	34.350*	mmol g ⁻¹	$V_{p\uparrow} =$	1.19×10^{-6}	m ³ g ⁻¹ ^(1,2)
$\langle \chi_{p\uparrow} \rangle =$	3.974	monolayers	$d^\# = 4V_{p\uparrow}/A_{p\uparrow} =$	16.8	nm ^(1,2)
$\langle \Delta \chi_{p\uparrow} \rangle =$	1.558*	monolayers	$t_m =$	0.709	nm ⁽²⁾
			$t = t_m \langle \Delta \chi_{p\uparrow} \rangle =$	2.82	nm ^(1,2)
			$\langle \bar{E}_{p\uparrow} \rangle =$	-136.6	J mol ⁻¹ ⁽¹⁾
			$r_c^{(\langle \bar{E}_{p\uparrow} \rangle) \dagger} =$	2.21	nm ^(E_{p\uparrow}, 2)
			$r^\uparrow = r_c + t =$	5.03	nm ^(1,2)
			$d_{p\uparrow} = 2r^\uparrow =$	10.06	nm
			$A_{BET} =$	580	m ² g ⁻¹
			$V^\# =$	1.42×10^{-6}	m ³ g ⁻¹
			$d = 4V^\#/A_{BET} =$	9.79	nm ⁽²⁾
			$d_{p\uparrow}^\#_{ads} =$	10.1	nm
$\sigma_p =$	6.989×10^{-2} *	monolayers	$\langle \bar{E}_{d\downarrow} \rangle =$	-270.8	J mol ⁻¹
$\sigma_{fit} =$	0.6127	mmol g ⁻¹	$\langle \Delta \chi_{d\downarrow} \rangle =$	3.11	
$\sigma\% \text{ FDR} =$	1.45 %				
* This indicates an output parameter.			FDR = “of Full Data Range”		
‡ Measured from admolecules’ centers					
† Measured across pore admolecules’ inside edges.					
# This datum is given by GWMTK using NLDFT ⁹ .					
$p_{d\downarrow}$ = desorption values from another spreadsheet for this sample					
<p><i>Note: The values for the pore diameter are in bold font. If the pores were perfect cylinders lone standing these should be correct, However, the lattice of the sample is 3-dimensional interconnected cylinders, and the values listed should be larger than the true diameter. The A_{BET} is higher than the QM calculation, and if the QM is correct, then the true value for A is about 2 to 3 greater than the listed value. That means, the it would have calculated to 20 to 30 nm. So, both the corrected BET and the QM cannot reliably calculate the pore radius by the ratio V/A. It obviously calculates another fractal quantity.</i></p>					

The first observation is that the $\sigma\% \text{ FDR}$ is slightly out of the acceptable range but, certainly better than any other type of fit to this entire isotherm. It appears there are T -control problems at

the beginning and there is uncertainty about $\langle \chi_c \rangle$. This will create uncertainty for the n_m and other vital parameters. However, this is for illustration of what to obtain from the isotherm, especially for the hysteresis.

Equation 5 can be related back to pressure and the χ -plot:

$$\bar{E}_p := \Delta_l^a \mathbf{E}(n_p) \cong -RT \ln \left(\frac{P_p}{P_{\text{vap}}} \right) = -\frac{m\gamma\bar{V}}{r_{\text{core}}} \quad \text{Equation 5}$$

In *Equation 5* P_p is the pressure at which the transition from the QM controlled adsorption to the classical gas-liquid interface. The approximate identity is due to the Dubinin "Thermodynamic criterion," (explained in Appendix II of Part V) but at this pressure the $\Delta_l^a S$ is relatively trivial. *Equation 5* can be used to calculate the core radius, r_c , and to obtain the pore radius the "thickness" of the layers inside the pore, t , must be added to this.

Obtaining the diameter of the pore by using the volume and surface area of the pores seems problematic. The volume to area ratio for the QM is quite high, but the sample is not perfect regular cylinders but rather a lattice of intersecting cylinders. Thus, the calculation from the E_p is a more reliable indication. Interpretation of the meaning of the ratio is another matter.

For the V/A ratio, the BET value of A_{BET} is undoubtedly too high*. Therefore, by coincidence, the calculation of the diameter is almost correct. This is assuming that the pores are perfect, isolated cylinders, which is unlikely. Since the BET yields an area that is about a factor of about 1.6 too high, the ratio V/A with a corrected A yields a pore diameter ~ 15.7 nm. Thus, both the modified BET and the QM yield values of diameter that are quite high compared SEMs and NLDFT.

On the other hand, the Kelvin equation is not dependent upon the total volume, but rather the radius of the pores. With this calculation, the QM calculation using t and r_c the value for the pore diameter is very close to the calculation by the NLDFT. Thus, using the BET, the ratio V/A calculates a pore diameter of about 20. This question should be addressed with data that is clearer for the calculation.

The difference between the V/A ratio and d may be a fractal measurement of some importance. More research is needed here.

This data is suitable to do another calculation, that is the calculation of the expected desorption isotherm from the adsorption isotherm. This question was examined in reference 3 and examined more closely here.

Speculation about calculating hysteresis:

The same data from the GWMTK of N_2 on S(140)24_N sample and the companion desorption data was used to test the idea that the parameter m switches from 1 for adsorption to 2 for desorption. Furthermore, the χ_c is reevaluated to determine if something fundamentally changes from adsorption to desorption, specifically if the adsorption of a pure adsorptive helps to clean

* See Part III for more precise calculation.

the adsorbent surface. This phenomenon was observed in the data by Silvestre-Albero, Silvestre-Albero, Llewellyn, and Rodríguez-Reinoso¹⁰ of He retention on carbon samples even after a normal degas cycle. There is no reason to expect that it does not apply here.

In *Table 3* are the output parameter of the non-linear least squares fit to both the adsorption and desorption using both the χ^{-1} and the **D** distributions

<i>Table 3</i> parameters from sample S(140)24 N by GWMTK using either χ^{-1} or G distributions				
Quantity	Adsorption - χ^{-1}	Adsorption - G	Desorption - χ^{-1}	Desorption - G
$n_{m,1} / \text{mmol g}^{-1} =$	3.979	4.028	4.474	5.592
$\chi_{\zeta} =$	-2.4163	-2.4506	-3.1012	-2.4600
$n_{m,\text{ext}} / \text{mmol g}^{-1} =$	1.071	2.648	1.072	1.098
$n_p / \text{mmol g}^{-1} =$	34.350	27.356	28.813	29.333
$\Delta\chi_p =$	3.974	3.982	4.015	3.381
$\sigma_p / \text{mmol g}^{-1} =$	6.989E-02	6.765E-02	2.347E-02	1.417E-02
$\sigma / \text{mmol g}^{-1} =$	0.61269	0.53659	0.52818	0.47154
$\sigma(\text{FDR}) =$	1.45%	1.27%	1.43%	1.28%
$\chi_p^\dagger =$	1.558	1.532	0.913	0.921
if $m =$	1	1		
$E_p^\dagger / \text{J mol}^{-1} =$	-136.6	-140.20		
if $m =$	2	2	2	2
$E_p^* / \text{J mol}^{-1} =$	-273.2*	-280.4*	-260.1	-258.3
$\chi_p^* =$	0.865*	0.839*	0.913	0.921
$\Delta^* E_p = E_p^\dagger - E_p^* =$	13.1 J/mol	22.1 J/mol	---	
$\Delta^* E_p / E_a =$	0.18 %	0.29%		
$\Delta^* \chi_p = (\chi_p^\dagger - \chi_p^*) =$	-0.048	-0.082	---	

† indicates when $m = 1$ * indicates if m were =2

Table 3 provides all the information to calculate the energy difference between the adsorption peak and the desorption peak energies for the GWMTK. If one assumes that the value for $m = 1$ for adsorption and $m = 2$ for desorption due to the difference in geometry of the gl interface (Fig 6.19³) the energy difference is a factor of about 17 J mol^{-1} (not kJ mol^{-1} !) In comparison of the starting value of the differential heat of adsorption in ~ -5 to -20 kJ mol^{-1} (in this case 7.27 kJ mol^{-1}) this is very trivial. The difference between adsorption and desorption compared to the E_a in this case amount to only $\sim 0.13\%$. If it were not for the stretching out of the usual isotherm representation at high pressures, this difference would hardly be noticed.

This, however, may still be significant and certainly more work needs to be performed to determine the possible causes of hysteresis.

Even though presently, the QM does not predict or explain hysteresis, the ESW hypothesis might. The ESW is based on forces rather than energy

Conclusion concerning mesoporosity:

So far, the QM/ESW hypothesis does an excellent job of fitting isotherms which include “simple case” and making modification for:

1. Heterogeneity
2. Microporosity and
3. Mesoporosity both adsorption and desorption and a potential start for
4. Hysteresis

The argument for the first three is very strong. For the fourth one, a lot more work is required. However, interpretation of the fitting parameters for mesoporosity is especially tentative for the phenomenon of hysteresis.

Another question, “What is the definition of pore size?” is not clear. More high-quality experimentation and theoretical development is clearly needed to determine a practical definition.

What is next?

But what so far has been neglected herein? – An important question to guide future research:

More work relating the heats of adsorption to the isotherm data is needed with the technique and with equipment at least as good as that by Berg. Although there is some data compiled in the literature¹¹, there is only one publication that does a direct measurement with the same sample in the same combined equipment^{12,13,14}. Much better controlled experiments are in order. As good as Berg’s data is, there are still questions about the actual calculations made, knowing that the differential heat is, by nature, missing one critical data point.

The use of QM/ESW as applied to binary adsorptives looks like it might be possible. The use of the Langmuir isotherm has been tried, with only modest success¹⁵. The biggest problem in the endeavor has been the involved mathematics required, but of course, the Langmuir is not appropriate for the full isotherm or the very low pressures. It is however a relatively simple equation for use in differential equations. The χ -transform would seem an easier route. Unfortunately, there does not seem to be enough basic research on even the simplest systems to start testing any derivation.

These two topics, along with an overall summary and conclusion, is presented in Part VII.

Appendix I about equations 1 and 2:

This appendix addresses some properties of *Equation 2* and *Equation 3*. Firstly, to assuage the doubts about these functions and secondly to provide some insight into their properties

$$F_1 = \exp \left\{ -\exp \left(-\frac{(x - \langle x_p \rangle)}{\sigma_p} \right) \right\} \quad \text{versus} \quad F_2 = -\exp \left\{ -\exp \left(-\frac{(\langle x_p \rangle - x)}{\sigma_p} \right) \right\} \quad \text{Equation 6}$$

Firstly, a definition: The “peak value” is the maximum of the first differential of the function being used to describe the mesopore filling. In a normal distribution, the peak value is at the value of the mean. This is not the case for the χ or χ^{-1} .

The limits for these equations are, at least theoretically, $x - x_p = -\infty$ to ∞ and the differential for both functions reach a peak at x_p . This is because the argument in the inner **exp** function is 0 and an inflection point is reached, like the Fuller magic point for the isotherm.

So, if $x - x_p = 0$, $F_1 = F_2$. Thus, the peak value is the same for the two functions. It is also the same for the normal distribution.

A) If $x - x_p = -\infty$, $F_1 = 0$ and $F_2 = -1$.

B) If $x - x_p = +\infty$, $F_1 = 1$ and $F_2 = 0$.

For F_1 what is listed makes sense. If one goes left on the usual isotherm representation the mesoporosity goes up. But what about F_2 ? Starting from the right on the diagram one should go down for hysteresis. So going from A) to B) there should be a decrease. So, the function in front of F_2 needs to express this. In other words, in *Equation 3* the functions $n_{a,f}$ and $n_{a,i}$ exchange places from *Equation 2*. Another way of looking at this is the mesopore function for the desorption is $(1 - F_2)$ if one goes from right to left on the diagram. $(1 - F_2)$ is the C_{2v} image of F_1 .

The characteristics of the χ , the χ^{-1} and the normal distributions are shown in *Figure 6*. A constant χ_c is assumed, which may not be the real case. The * indicates the mirror image

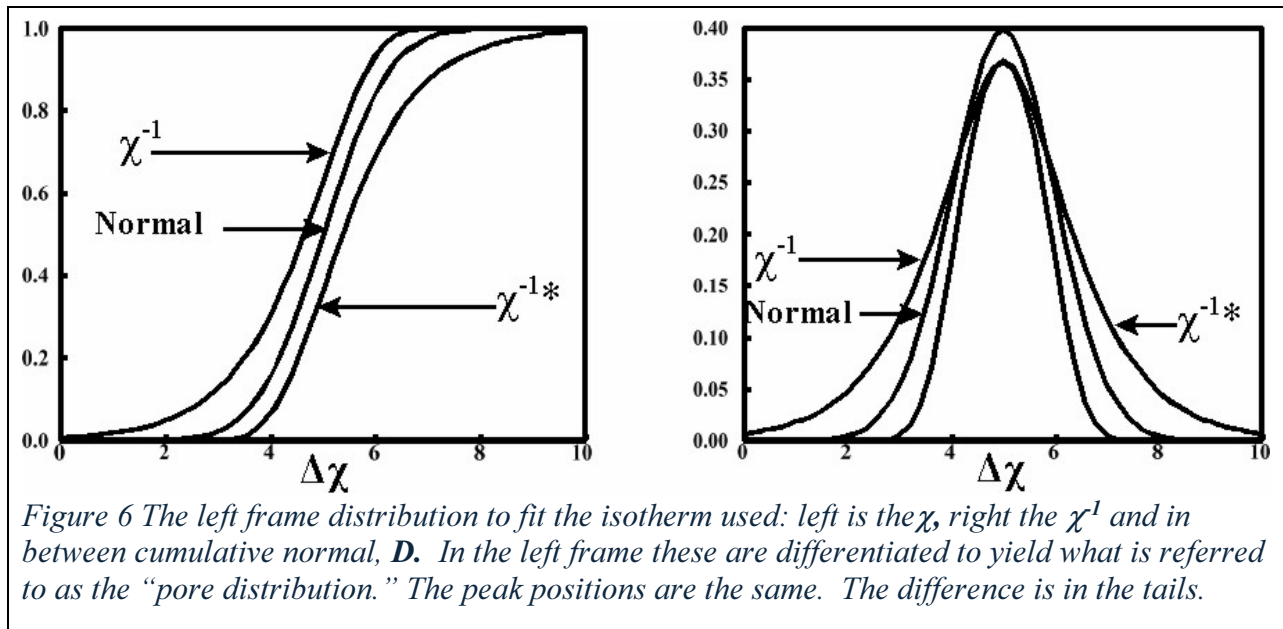


Figure 6 The left frame distribution to fit the isotherm used: left is the χ , right the χ^{-1} and in between cumulative normal, **D**. In the left frame these are differentiated to yield what is referred to as the “pore distribution.” The peak positions are the same. The difference is in the tails.

Acknowledgements:

I am thankful for the guidance received from Dr. E. Loren Fuller, Jr., who was a kind mentor to me and passed on the knowledge that started with Polanyi. I am grateful to W. Thomas Berg who provided me with his excellent thermodynamic data that provided a significant breakthrough. I also wish to thank Dr. Jürgen Adolphs for his encouragement, multiple discussions and confirmatory evidence for the theoretical developments.

Funding:

This article was not funded.

Data and materials availability:

All the data and materials are available in the open literature and are referenced herein.

References:

-
- ¹ J. B. Condon, Using classical methods to start quantum mechanical calculations for microporosity and mesoporosity. *Adsorption* **26**, 1291–1299 (2020).
 - ² R. Guillet-Nicolas, M. Wainer, L. Marcoux, M. Thommes, F. Kleitz, J. Insights into pore surface modification of mesoporous polymer-silica composites: Introduction of reactive amines. *Colloid Interface Sci.* **579**, 489–507 (2020)
 - ³ J. B. Condon, *Surface Area and Porosity Determinations by Physisorption, Measurements, Classical Theories and Quantum Theory* (Elsevier, Amsterdam ed.2 fig. 6.19, 2020).
 - ⁴ UNIFAC, “Modified UNIFAC (Dortmund) and the Predictive Equations of State PSRK and VTP” http://unifac.ddbst.de/en/EED/PCP/SFT_C1056.php - also see: (Dortmund Data Base, DDB #1057, Nitrogen, CAS = 7727-37-9.)
 - ⁵ M. Thommes, K. Kaneko, A. V. Neimark, J. P. Olivier, F. Rodriguez-Reinoso, J. Rouquerol, K. S. W. Sing, Physisorption of gases, with special reference to the evaluation of surface area and pore size distribution (IUPAC Technical Report), *Pure Appl. Chem.*, **87(9-10)** 1051–1069 (2015).
 - ⁶ K. S. W. Sing, D. H. Everett, R.A.W. Haul, L. Moscou, R. A. Pierotti, J. Rouquerol, T. Siemieniewska, **Error! Main Document Only**. International Union of Pure and Applied Chemistry, Physical Chemistry, commission on Colloid and Surface Chemistry Including Catalysis, Reporting Physisorption Data for Gas/Solid Systems with Special Reference to the Determination of Surface Area and Porosity. *Pure & Appl. Chem.* **57(3)**, 603-619 (1985).
 - ⁷ S. Brunauer, *The Adsorption of Gases and Vapor - Volume 1 Physical Adsorption* (Princeton University Press, 1942),(Oxford University Press, 1946) p194 in the Legare Street Press release.

- ⁸ W. E. Fuller Jr.,— Private discussion with S. Brunauer requested by JBC.
- ⁹ P.I. Ravikovitch, A.V. Neimark, Characterization of Micro- and Mesoporosity in SBA-15 Materials from Adsorption Data by the NLDFIT Method. *J. Phys. Chem. B*, **105** 6817–6823 (2001).
- ¹⁰ J. Silvestre-Albero, A. M. Silvestre-Albero, Philip L. Llewellyn, and Francisco Rodríguez-Reinoso, High-Resolution N₂ Adsorption Isotherms at 77.4 K: Critical Effect of the He Used During Calibration. *J. Phys. Chem. C*, **117** 16885–16889 (2013).
- ¹¹ J.B. Condon, **Error! Main Document Only**.Heats of physisorption and the predictions of chi theory. *Microporous Mesoporous Mat.* **33**, 21-36 (2002).
- ¹² W. T. Berg, “Heat Capacities from 15-140 K and Entropies of Krypton Adsorbed On Anatase,” PhD Thesis, Western Reserve University (now Case Western Reserve University) Cleveland, OH, USA (1955)
- ¹³ E. L. Pace, K. S. Dennis, W, T, Berg, **Error! Main Document Only**.Thermodynamic properties of krypton adsorbed on titanium dioxide (rutile). *J. Chem. Phys.* **23**, 2166-2168 (1955).
- ¹⁴ E. L. Pace, W, T, Berg, A. R. Siebert, Entropy of Krypton Adsorbed on Titanium Dioxide (Anatase). *J. Am. Chem. Soc.* **78(8)**, (1956) 1531-1533.
- ¹⁵ D. Basmajian, *The Little Adsorption Book*, (CRC Press, Inc. Boca Raton FL, USA,1996) ISBN 0-8493-2692-3